Stem Cell Reports, Volume *16*

Supplemental Information

Cell-to-Cell Adhesion and Neurogenesis in Human Cortical Development: A Study Comparing 2D Monolayers with 3D Organoid Cultures

Soraya Scuderi, Giovanna G. Altobelli, Vincenzo Cimini, Gianfilippo Coppola, and Flora M. Vaccarino

Cell-to-cell adhesion and neurogenesis in human cortical development: a study comparing 2D monolayers with 3D organoid cultures

Soraya Scuderi[1,5], Giovanna G. Altobelli[1,2,5], Vincenzo Cimini[2], Gianfilippo Coppola[1,4,*], Flora M. Vaccarino[1,3,*]

Supplemental Experimental Procedures

Neuronal Differentiation of hiPSC lines. Noggin protocol. We differentiated three human male control iPSC cell lines (07-01#1, 1123-01#3, 1120-01#7) into telencephalic neurons according to our established method (Mariani et al., 2015). Human iPS cells were dissociated to single cells with Accutase (Chemicon), and a total of 3.2 million cells was plated in AggreWell™ 800 plates and cultured in DMEM/F12-GLUTAMAX (neuronal medium) with 4% B27 without vitamin A, 1% N2 and supplemented with recombinant mouse Noggin (R&D Systems 1967-NG-025) and Y-27632. After 2 days, embryoid bodies (EBs) were collected and plated onto 10-cm bacterial Petri dishes in neuronal medium as above with the addition of B27 supplemented with vitamin A**,** Y-27632 and Noggin. On Day 4, free-floating EBs were collected and plated in neuronal medium, supplemented with only Noggin, onto 10 cm tissue culture dishes coated with growth factor-reduced Matrigel (BD Bioscience, diluted 1:30 with DMEM:F12 medium) to allow neural rosette formation. The next day (day 5), the neuronal medium was changed and supplemented with 20 ng/ml FGF2, 200 ng/ml Noggin, and 200 ng/ml rhDkk1 (R&D Systems, 5439-DK). After two or three days the neural rosettes were manually dissected and replated as free-floating aggregates in 10-cm bacterial Petri dishes in neuronal medium supplemented with FGF2 (10 ng/ml) and EGF (10 ng/ml). For the dissociation followed by immediate re-aggregation (REAG) and monolayer (MON) culture conditions, after 4 days in suspension, neuronal rosettes were dissociated to single cells with Accutase and quickly re-aggregated (20,000 cells) in a low cell adhesion 96 well plate (REAG), or plated (30,000 cells/0.8cm^2) onto poly-L-ornithine and laminin coated 8 well permanox chamber slides (Thermo Scientific) as adherent monolayer cultures (MON). Alternatively, for the organoid (ORG) condition, free-floating aggregates were left undissociated (see **Figure 1A**). All preparations were kept in the same neuronal medium supplemented with FGF2 and EGF for another day. The next day all preparations were transferred in growth factor-free neurobasal-type medium supplemented with BDNF (R&D), GDNF (R&D), ascorbic acid, and dibutyryl-cAMP (Sigma). This medium change triggers the onset of terminal differentiation (TD) and thus, this day is indicated TD day 0 (TD 0). **Dual SMAD inhibition protocol.** The same three iPSC lines were differentiated into cortical neurons by using a modified version of the Dual-SMAD neuronal induction protocol of Rigamonti et al.,2016 (Rigamonti et al., 2016), that use SB431542 and LDN-193189 in place of Noggin. Media used were: *mTeSR™ Plus* (STEMCELL Technologies, #100-0276); *KSR medium*: 15% KSR (Invitrogen), KO DMEM (Invitrogen), L-glutamine (Gibco), 100X non-essential amino acids (NEAA) (Gibco), 100X penicillin-streptomycin (Gibco), and 1000X b-mercaptoethanol (Gibco); *Neural induction medium* (NIM): DMEM/F12 (Invitrogen), 100X N2 supplement (Gibco), 50X B27 supplement without vitamin A (Life Technologies),100X Glutamax (Gibco), 100X NEAA (Gibco), 100X penicillin-streptomycin (Gibco), 0.15% D-(+)-Glucose solution (Sigma G8644). Human iPSCs were dissociated by Accutase into a single cells suspension (day 0), and a total of 4 million cells was plated into a well of 6-multiwell plate and rotated on an orbital shaker (Labstrong) at 95 RPKM in mTeSR™ Plus medium with Y-27632 (5 μM) in a 37°C, 5% CO2. On day 2, the medium was replaced with fresh mTeSR™ Plus medium. At day 3 of differentiation, medium was changed to mTeSR with SB431542 (R&D Systems,10 mM) and LDN193189 (Stemgent,1 mM) (referred as Dual-SMAD inhibition). From day 4 to day 11 EBs were gradually adapted to neuronal induction medium (NIM) through a dilution series of KSR and NIM in the presence of Dual-SMAD inhibition throughout. Medium was changed as follows: day 4: 100% KSR medium with Wnt signaling inhibitor XAV939 (2 mM) (Stemgent); day 7: 75% KSR medium, 25% NIM; day 9: 50% KSR medium, 50% NIM; day 11: 25% KSR medium, 75% NIM. From days 13 to 18, cultures were maintained in 100% NIM supplemented with FGF2 (10 ng/ml) and EGF (10 ng/ml). From day 19 onward, cultures were maintained in neurobasal medium neurobasal-type medium supplemented with BDNF (R&D), GDNF (R&D), ascorbic acid, and dibutyryl-cAMP (Sigma). This medium change triggers the onset of terminal differentiation (TD) and thus, this day is indicated TD day 0 (TD 0). Re-aggregated culture (REAG) and monolayer (MON) conditions were generated in the same way as described above with the Noggin protocol at day 19 (TD0) where neuronal progenitor cells in EBs have organized themselves in rosettes structures evident at the brightfield microscope.

To examine the role of laminin/β1-ITG signaling, rosettes (obtained from hiPSC line 1123-01#3) were dissociated and plated as monolayer on Poly-l-ornithine/laminin, as described before, and grown for 2 (TD2) or 11 days (TD11),

with the addition of either 2μg/ml of IgG2bk Functional Grade Isotype Control (Thermo Fisher cat number 16-4732-85) or 2μg/ml of monoclonal antibody IgG2bk anti-human β1integrin (MilliporeSigma, MAB1959Z).

Immunofluorescence and stereological analysis. Organoids and reaggregates were fixed in 4% PFA for 3 hours, washed three times in PBS1X and transferred in 30% sucrose overnight at 4ºC, then embedded in OCT and cryosectioned at 14 μm. Monolayers were fixed in 4% PFA for 3 hours and washed three times in PBS1X. Cryosections or monolayers culture wells were blocked in 10% normal donkey serum (NDS)/0.1% Triton X-100/PBS for 1 hour at room temperature and incubated overnight at 4ºC with primary antibody diluted in a solution containing 5% NDS/0.05% Triton X-100/PBS. Sections were washed in PBS/0.1% Triton X-100 3 times and incubated for 1 hour with a secondary antibody diluted in 5% NDS/0.05% Triton X-100/PBS. Primary antibodies were as follows: goat anti-Sox1 (1:20; R&D Systems, AF 3369), mouse anti-Pax6 (1:200; BD Biosciences, 561462), mouse anti TUBB3 (1:1000; Promega, G712A), rabbit anti-Ki67 (1:500; Vector, VP-RM04), rabbit anti Tbr1 (1:1000; Abcam, ab31940), rat anti Citp2 (1:500; Abcam, 18465), rabbit anti GABA (1:500; Millipore, A2052), mouse anti GAD1/GAD67 (1:1000; Millipore, MAB5406), rat anti CTIP2/BCL11B (1:500; Abcam, ab18465), mouse anti β-Catenin (1:100; BD Transduction Laboratories, 610153), mouse anti-N-Cadherin (1:500; BD Transduction Laboratories, 610920). Nuclei were stained with DAPI. All images were acquired using an ApoTome-equipped Axiovert 200M with Axiovision 4.5 software. Quantification of immunostained cells was performed by stereological analysis using a Carl Zeiss Axioskop 2 Mot Plus, connected to a computer running Stereoinvestigator Software (MicroBrigh-Field) as previously described (Mariani et al., 2015).

Western Blot analysis. Western blot analysis was performed to determine protein expression levels as previously described (Scuderi et al., 2013). Samples were suspended in RIPA cell lysis buffer (Millipore 20-188) supplemented with Protease and Phosphatase inhibitor cocktail (Roche Diagnostics) and homogenized by using a teflon-glass homogenizer, then sonicated twice for 20 sec using an ultrasonic probe, followed by centrifugation at 10,000 g for 20 min at 4 °C. Protein concentration was determined by the Qubit Protein Assay Kit (Invitrogen). Samples (30 μg each) were diluted in 2X Laemmli buffer (Invitrogen, Carlsbad, CA, USA), denatured at 70°C for 10 min and proteins were separated on a Biorad Criterion XT 4-15% Bis-tris gel (BIO-RAD) by electrophoresis and then transferred to a nitrocellulose membrane (BIO-RAD). Blots were blocked using 5% bovine serum in Tris-buffered saline with 0.1% Tween 20 and probed with the following antibodies: 1:500 rabbit anti-TBR1 (cat n. 31940, Abcam), 1:500 rabbit anti-DCX antibody (cat n. 18723, Abcam), 1:200 goat anti-Neurogenin2 (cat n. SC19233, Santa Cruz Biotechnology), 1:500 mouse anti-GAPDH (cat n. MAB374 Millipore), 1:1000 rabbit anit-FAK (cat n. #3285, Cell Signaling), 1:1000 rabbit anti-Phospho-FAK(cat n. #8556, Cell Signaling). An anti-rabbit IgG HRP-linked antibody (cat #7074; Cell Signaling) or an anti-mouse IgG HRP-linked Antibody (cat #7076; Cell Signaling) or anti-goat IgG HRP-linked Antibody (cat n. 705-035-003 Jackson ImmunoResearch) were used. Blots were visualized using SuperSignal West Pico Chemioluminescent Substrate (Thermo Scientific, 34080), gels were quantified by using ImageJ (NIH) (Schindelin et al., 2012).

RNA isolation and RNA sequencing experiments. Total cellular RNA was collected from intact organoids and reaggregates (about 15-20 organoids for each line), and from two 9 cm^2 wells of a 6 wells plate for a monolayer culture at TD 2, TD 11 and TD 31 and purified using PicoPure RNA isolation kit (Applied Biosciences) as per manifacturer's instructions. Poly(A)+ RNA from 3 biologically different iPSC lines per condition (ORG, REAG and MON) was used as template for the preparation of 27 human cDNA libraries, which were then subject to single end RNA seq.

Quantitative real time RT-PCR. An aliquot of the Poly(A)+RNA from ORG, REAG and MON that was previously used for RNAseq analysis, was used for secondary validation through real-time PCR analysis. Our analysis revealed a correlation coefficient of 0.77 between log2 (fold changes) in expression from the two techniques. 10 ng of RNA was used for cDNA synthesis using SuperScript III First-strand synthesis Supermix and random hexamers (Invitrogen, #1808-051). Primers for 34 randomly picked differentially expressed genes were designed using NCBI/Primer-BLAST (**Table S3e**). PCR reactions were conducted on a StepOnePlus Real-Time PCR System (Applied Biosystems) by using a SYBR-green based method (Fast SYBR Green Master Mix, ABI) followed by melt curve analysis to verify specificity of the product. The Ct value was used to calculate the relative amount of mRNA molecules. The Ct value of each target gene was normalized by subtraction of the Ct value from GAPDH housekeeping genes to obtain the ΔCt value.

Statistical Analysis. Statistical analysis of cell counts, qPCR and Western blot assays was performed using GraphPad Prism Version 7 (GraphPad Software, USA). Significance was determined by Student t-test or ANOVA as indicated in figure legends. Results are expressed as mean ± SEM.

RNAseq data analysis. Sequencing reads were mapped to the human genome (hg19) and the GencodeV7 (Harrow et al., 2012) transcriptome annotation. The BEDtools function coverageBed (Quinlan and Hall, 2010) was used to estimate gene expression as counts. The R package edgeR (Robinson et al., 2010) was used to estimate gene expression as RPKM.

Differential expression analysis. Differentially expressed genes were inferred using the edgeR pipeline (Robinson et al., 2010), using the trended dispersion to estimate the biological variance. In one instance, where blocking by line would result in an N=1, we blocked by batch to have N=2 (see **Table S1a**). We contrasted cell culture models (i.e. MON vs ORG) and developmental time points (i.e. TD11 vs TD2 and TD31 vs TD11). Within each contrast, counts data were first filtered, by requiring that at least 50% plus one of the samples have a level of expression of 1 count per million or more. About 17000-20000 genes survived the filter and were further processed. Nominal p-values from differential expression analysis were FDR corrected, and an FDR cut-off of 0.05 was used for all the tests. Functional enrichment analysis. ConsensusPathDB (Kamburov et al., 2011) was used to test differentially expressed genes for overrepresentation in Gene Ontologies and Canonical Pathways.

Weighted gene co-expression network analysis. We used Weighted Gene Co-expression Network Analysis (WGCNA) (Langfelder and Horvath, 2008) for co-expression network analysis using gene expression estimates (as log2(RPKM+1)) from all the hiPSCs derived organoids (3 cell lines and 3 time points). We then estimated the co-expression network and modules using the function blockwiseModule with the following parameters: maxBlockSize=30000; corType=bicorr; power=30; networkType=signed; deepSplit=2; minModuleSize=50.
The analysis produced a network of 42 modules, corresponding to about 20214 genes, including the grey module of unassigned genes (**Table S6**). We used permutation analysis to verify that the modules identified were not artifacts of the clustering procedure. We assumed the mean topological overlap of a network module to be greater than the mean topological overlap of a random set of genes, in order for the module genes to be co-expressed beyond chance. For each module we estimated the average topological overlap (Langfelder and Horvath, 2008), then randomly selected a number of genes equal to the number of module members and estimated the corresponding mean topological overlap. This operation was repeated 100 times. The p-value for the analysis was estimated by dividing the number of times the mean topological overlap of the random set of genes was greater than that of the network module, by the number of permutations (N=100). Finally, the p-values for all the modules were FDR corrected for multiple comparisons, and a cut-off of 0.05 was considered for significance. All the modules passed the test and were considered for further analysis. Correlation analysis of modules' eigengenes was used to highlight module to module relationship (**Table S6**). We used ConsensusPathDB (Kamburov et al., 2011) for functional annotation of modules.

Transcription factor analysis. We inferred transcription factors (TFs) potentially upstream of genes within the blue module using the EnrichR online database (Kuleshov et al., 2016) and retained only statistically significant TFs at a fdr corrected p-value of 0.05. We then filtered out TFs whose target genes do not show overlap with the MON vs ORG DEGs list at all time points. This ensures that inferred TFs with no clear sign of activity are removed from downstream analysis. Next, we downloaded the Neurogenesis and the GO_CELL_CELL_ADHESION gene sets from the Broad Institute MSigDB (v6.2) collection (Liberzon et al., 2011; Subramanian et al., 2005). Then, we tested each TF-target for statistical overlap with the Neurogenesis gene set, and the resulting set was then tested for overlap with the cell-cell adhesion gene set. We retained only TFs showing overlap with both gene set at an FDR<0.05. We integrated the TF-target genes directed relationships derived from literature, with our undirected WGCNA network edges. This resulted in a directed network, with data driven edges strength (i.e. correlation coefficient), where non relevant edges (i.e. edges with zero correlation coefficients) could be filtered out. The resulting directed network highlights the regulatory relationship between the TFs that are upstream from the blue module and their target genes. Next, we estimated a weighted connectivity within this network, ranked the TFs in order of decreasing weighted connectivity. The resulting directed network highlights the regulatory relationship between the TFs that are upstream from the blue module and their target genes (**see Figure 6D**).

Creation of the neurodevelopmental genes list. We manually curated a neurodevelopmental list of genes by selecting group of genes whose function and expression has been previously described in published data from human

cortical developmental studies (Amiri et al., 2018; de la Torre-Ubieta et al., 2018; Hu et al., 2017; Johnson et al., 2015; Kang et al., 2011; Nowakowski et al., 2017; Pollen et al., 2014; Thomsen et al., 2016) and based on their annotation in existing datasets (KEGG pathway, HUGO Gene Nomenclature Committee). The neurodevelopmental genes list (**Table S4**) consists of the sublist Neuronal cell fate genes (168 genes), Cell Adhesion Molecules (247 genes) Axon Guidance (175 genes) and Extracellular Matrix (86 genes). We use this curated gene list to characterize the biological processes underlying the differences in gene expression among the ORG, MON and REAG conditions. For each comparison (e.g. MON vs ORG, REAG vs ORG) at each time point analyzed (TD2, TD11 TD 31), the log2(FC) of a DEGs of a specific category (sublists in **Table S4**) were collected into a data matrix, where each row represented one gene and each column represents one time point. After the matrix was created, a heat map plot was created by using GraphPadPrism Version 7 (GraphPad Software, USA).
We also interrogated a Dorsal-ventral forebrain Human Gene list obtained from the Human BRAINSPAN Developmental transcriptome (http://www.brainspan.org/rnaseq/search/index.html) by using differential search of target vs contrast structure and selecting human dorsolateral prefrontal cortex (DFC) vs basal telencephalon (e.g. lateral ganglionic eminence (LGE), medial ganglionic eminence (MGE), caudal ganglionic eminence (CGE), Striatum (STR)) and viceversa to obtain lists of up- or down-regulated genes in cortex and ventral telencephalon, respectively. The developmental stages selected were 8-9PCW, 10-12PCW and 13-15PCW, considering that ORG, the reference condition, best matches these human brain developmental stages (Amiri et al., 2018).

Mass Spectrometry (LC MS/MS)

Human iPSC derived neurons frozen cell pellets from ORG and MON at TD25 (2 iPSC lines, 07-01 and 1120), were lysed with RIPA buffer containing a protease and phosphatase inhibitor cocktail and with ultra-sonication (10% Amplitude, with 15 sec followed by 1 sec burst twice). Cellular debris were removed after centrifugation at 14,600g for 10 minutes at 4°Celsius. 100 µL of the supernatant was transferred to a new tube and proteins were precipitated with Chloroform:MeOH:water (100:400:300 µL). Protein pellets were washed three times with cold methanol prior to air drying for 5 minutes, and stored at -80°C. Dried protein pellets were resolubilized with 8M urea containing 400mM ammonium bicarbonate, reduced with dithiothreitol (DTT) at 37°C for 30 minutes, alkylated with iodoacetamide (IAN) at room temperature for 30 minutes in the dark, and then trypsin (1:50 enzyme:protein) digested twice, at 37°C overnight and at 37°C for 4 hours. Digestion was quenched with 20% trifluoroacetic acid, desalted using C18 reverse phase macrospin columns (The Nest Group Inc., Southborough, MA), and eluted peptides were dried using SpeedVac. Total peptides amount was determined by nanodrop (Thermo Fisher Scientific; Waltham, MA) High resolution tandem mass spectrometry was carried out on a Thermo Fisher Scientific Q-Exactive Plus connected to a UPLC system (Waters nanoACQUITY) equipped with a Waters Symmetry® C18 180 µm × 20 mm trap column and a 1.7-µm, 75 µm × 250 mm nanoACQUITY UPLC column (35°C). For additional details on UPLC and mass spectrometer conditions see (Goel et al., 2018). The LC-MS/MS data was processed using Proteome Discoverer (v2.1; Thermo Fisher Scientific) and protein identification was carried out using the Mascot search algorithm (Matrix Science). The Scaffold proteome software suite (ver 4.1.1) was used to estimate peptide/peptide groups, resulting in the identification of 21,597 peptide/peptide groups. Differential expression between MON and ORG, was then inferred using the Scaffold 4 Q+ module with default parameters (Precursor Intensity and Centroided Peak Intensity) to infer protein expression levels, using 99.0% minimum and 2 peptides minimum for protein threshold, 95.0% minimum for peptide threshold) and the Mann-Whitney Test for differential expression and FDR < 0.05 as significance levels. The resulting 199 differentially expressed proteins were used for functional annotation and subsequent analysis.

Supplemental References

Amiri, A., Coppola, G., Scuderi, S., Wu, F., Roychowdhury, T., Liu, F., Pochareddy, S., Shin, Y., Safi, A., Song, L., *et al.* (2018). Transcriptome and epigenome landscape of human cortical development modeled in organoids. Science *362*.

de la Torre-Ubieta, L., Stein, J.L., Won, H., Opland, C.K., Liang, D., Lu, D., and Geschwind, D.H. (2018). The Dynamic Landscape of Open Chromatin during Human Cortical Neurogenesis. Cell *172*, 289-304 e218.

Goel, R.K., Meyer, M., Paczkowska, M., Reimand, J., Vizeacoumar, F., Vizeacoumar, F., Lam, T.T., and Lukong, K.E. (2018). Global phosphoproteomic analysis identifies SRMS-regulated secondary signaling intermediates. Proteome Sci *16*, 16.

Harrow, J., Frankish, A., Gonzalez, J.M., Tapanari, E., Diekhans, M., Kokocinski, F., Aken, B.L., Barrell, D., Zadissa, A., Searle, S., *et al.* (2012). GENCODE: the reference human genome annotation for The ENCODE Project. Genome Res *22*, 1760-1774.

Hu, J.S., Vogt, D., Sandberg, M., and Rubenstein, J.L. (2017). Cortical interneuron development: a tale of time and space. Development *144*, 3867-3878.

Johnson, M.B., Wang, P.P., Atabay, K.D., Murphy, E.A., Doan, R.N., Hecht, J.L., and Walsh, C.A. (2015). Single-cell analysis reveals transcriptional heterogeneity of neural progenitors in human cortex. Nat Neurosci *18*, 637-646.

Kamburov, A., Pentchev, K., Galicka, H., Wierling, C., Lehrach, H., and Herwig, R. (2011). ConsensusPathDB: toward a more complete picture of cell biology. Nucleic Acids Res *39*, D712-717.

Kang, H.J., Kawasawa, Y.I., Cheng, F., Zhu, Y., Xu, X., Li, M., Sousa, A.M., Pletikos, M., Meyer, K.A., Sedmak, G., *et al.* (2011). Spatio-temporal transcriptome of the human brain. Nature *478*, 483-489.

Kuleshov, M.V., Jones, M.R., Rouillard, A.D., Fernandez, N.F., Duan, Q., Wang, Z., Koplev, S., Jenkins, S.L., Jagodnik, K.M., Lachmann, A., *et al.* (2016). Enrichr: a comprehensive gene set enrichment analysis web server 2016 update. Nucleic Acids Res *44*, W90-97.

Langfelder, P., and Horvath, S. (2008). WGCNA: an R package for weighted correlation network analysis. BMC Bioinformatics *9*, 559.

Liberzon, A., Subramanian, A., Pinchback, R., Thorvaldsdottir, H., Tamayo, P., and Mesirov, J.P. (2011). Molecular signatures database (MSigDB) 3.0. Bioinformatics *27*, 1739-1740.

Mariani, J., Coppola, G., Zhang, P., Abyzov, A., Provini, L., Tomasini, L., Amenduni, M., Szekely, A., Palejev, D., Wilson, M., *et al.* (2015). FOXG1-Dependent Dysregulation of GABA/Glutamate Neuron Differentiation in Autism Spectrum Disorders. Cell *162*, 375-390.

Nowakowski, T.J., Bhaduri, A., Pollen, A.A., Alvarado, B., Mostajo-Radji, M.A., Di Lullo, E., Haeussler, M., Sandoval-Espinosa, C., Liu, S.J., Velmeshev, D., *et al.* (2017). Spatiotemporal gene expression trajectories reveal developmental hierarchies of the human cortex. Science *358*, 1318-1323.

Pollen, A.A., Nowakowski, T.J., Shuga, J., Wang, X., Leyrat, A.A., Lui, J.H., Li, N., Szpankowski, L., Fowler, B., Chen, P., *et al.* (2014). Low-coverage single-cell mRNA sequencing reveals cellular heterogeneity and activated signaling pathways in developing cerebral cortex. Nat Biotechnol.

Quinlan, A.R., and Hall, I.M. (2010). BEDTools: a flexible suite of utilities for comparing genomic features. Bioinformatics *26*, 841-842.

Rigamonti, A., Repetti, G.G., Sun, C., Price, F.D., Reny, D.C., Rapino, F., Weisinger, K., Benkler, C., Peterson, Q.P., Davidow, L.S., *et al.* (2016). Large-Scale Production of Mature Neurons from Human Pluripotent Stem Cells in a Three-Dimensional Suspension Culture System. Stem cell reports *6*, 993-1008.

Robinson, M.D., McCarthy, D.J., and Smyth, G.K. (2010). edgeR: a Bioconductor package for differential expression analysis of digital gene expression data. Bioinformatics *26*, 139-140.

Schindelin, J., Arganda-Carreras, I., Frise, E., Kaynig, V., Longair, M., Pietzsch, T., Preibisch, S., Rueden, C., Saalfeld, S., Schmid, B., *et al.* (2012). Fiji: an open-source platform for biological-image analysis. Nat Methods *9*, 676-682.

Scuderi, S., D'Amico, A.G., Castorina, A., Imbesi, R., Carnazza, M.L., and D'Agata, V. (2013). Ameliorative effect of PACAP and VIP against increased permeability in a model of outer blood retinal barrier dysfunction. Peptides *39*, 119-124.

Subramanian, A., Tamayo, P., Mootha, V.K., Mukherjee, S., Ebert, B.L., Gillette, M.A., Paulovich, A., Pomeroy, S.L., Golub, T.R., Lander, E.S., *et al.* (2005). Gene set enrichment analysis: a knowledge-based approach for interpreting genome-wide expression profiles. Proc Natl Acad Sci U S A *102*, 15545-15550.

Thomsen, E.R., Mich, J.K., Yao, Z., Hodge, R.D., Doyle, A.M., Jang, S., Shehata, S.I., Nelson, A.M., Shapovalova, N.V., Levi, B.P.*, et al.* (2016). Fixed single-cell transcriptomic characterization of human radial glial diversity. Nat Methods *13*, 87-93.

Figure S1 (Related to Figure 1).

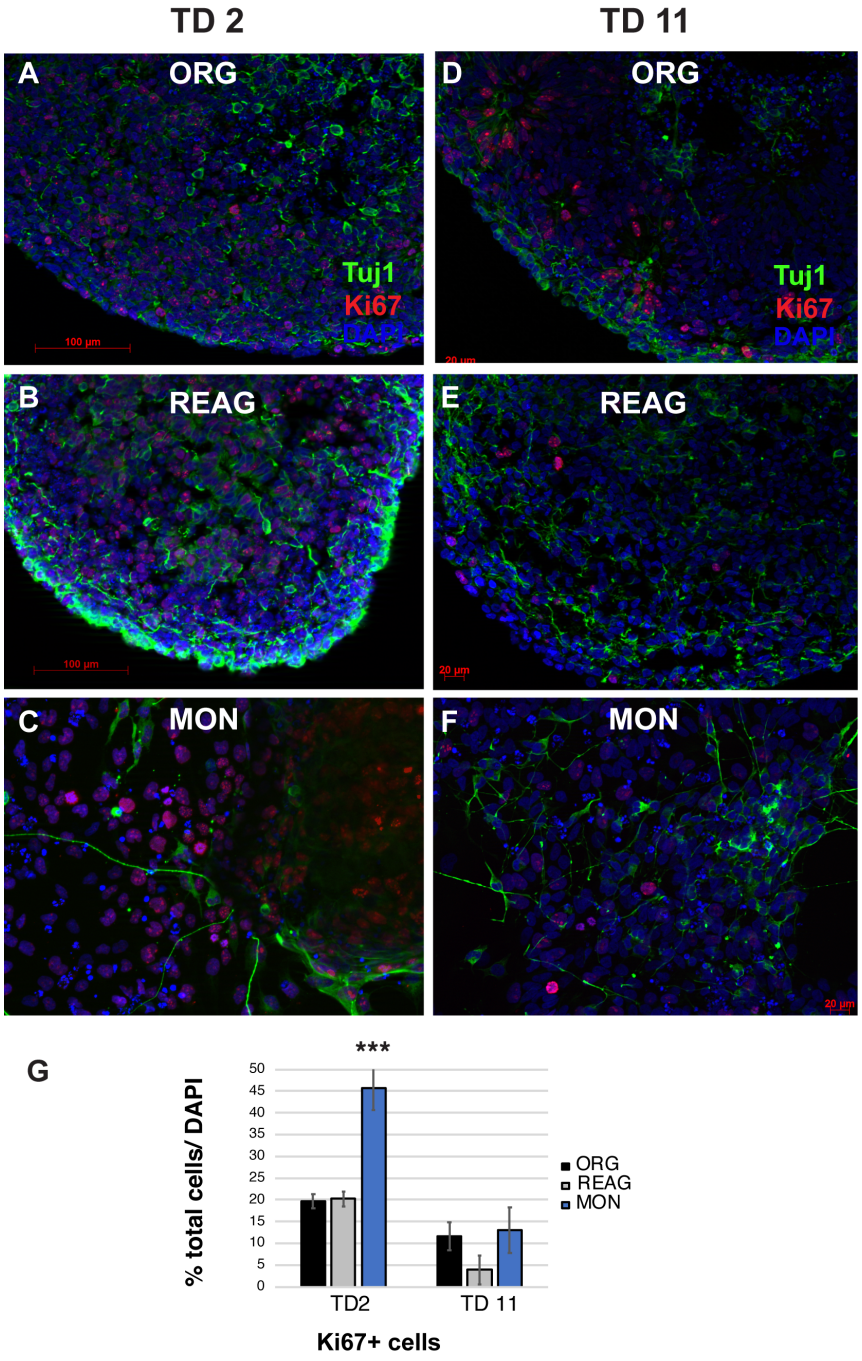

Figure S1. A-F, Representative images of immunocytochemical staining with the proliferative marker Ki67 and the neuron-specific class TUJ1 in ORG, REAG and MON preparations at TD 2 (**A-C**) and TD 11 (**D-F**). G, Proportion of $Ki67^+$ cells by stereological quantification over $DAPI^+$ nuclei. Results in (**G**) are the mean± SEM of n=3 biologically different iPSC lines per condition (ORG, REAG, MON) differentiated in parallel (one preparation each). For each preparation, 3 technical replicates (individual organoids, reaggregates or tissue culture wells) were analyzed. ***$p<0.001$ analyzed by Student's t-test, two tailed. Related to **Figure 1**.

Figure S2 (Related to Figure 3 and Table S4).

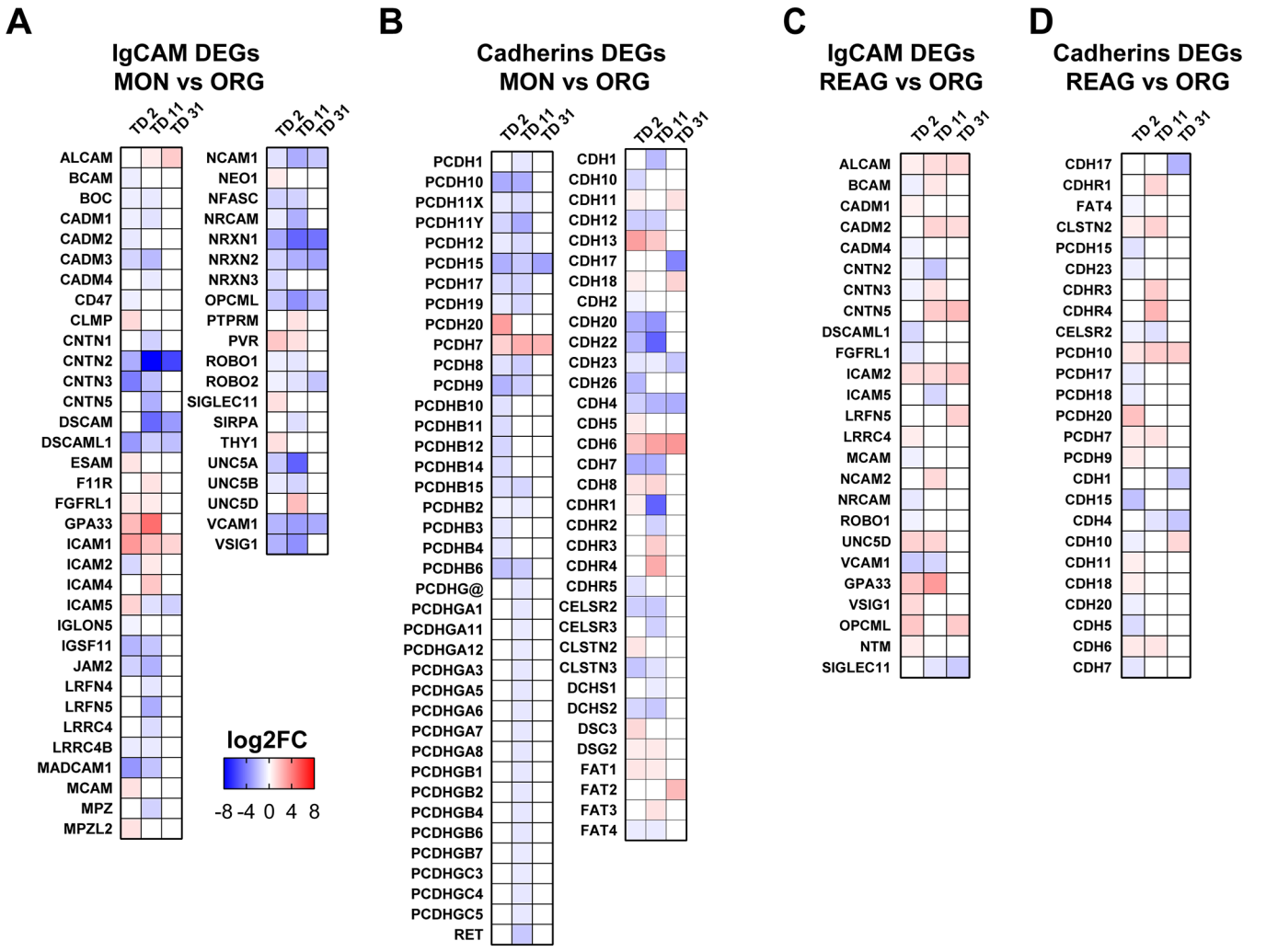

Figure S2. (A-D) Heat map of genes in the *Cell Adhesion* sublist (Table S4b) exhibiting differential gene expression (log2 fold change values, FDR<0.05) between MON and ORG (A-B), or between REAG vs ORG (C-D) at least at one time point analyzed. Related to **Figure 3** and **Table S4.**

Figure S3 (Related to Figure 3 and Table S4).

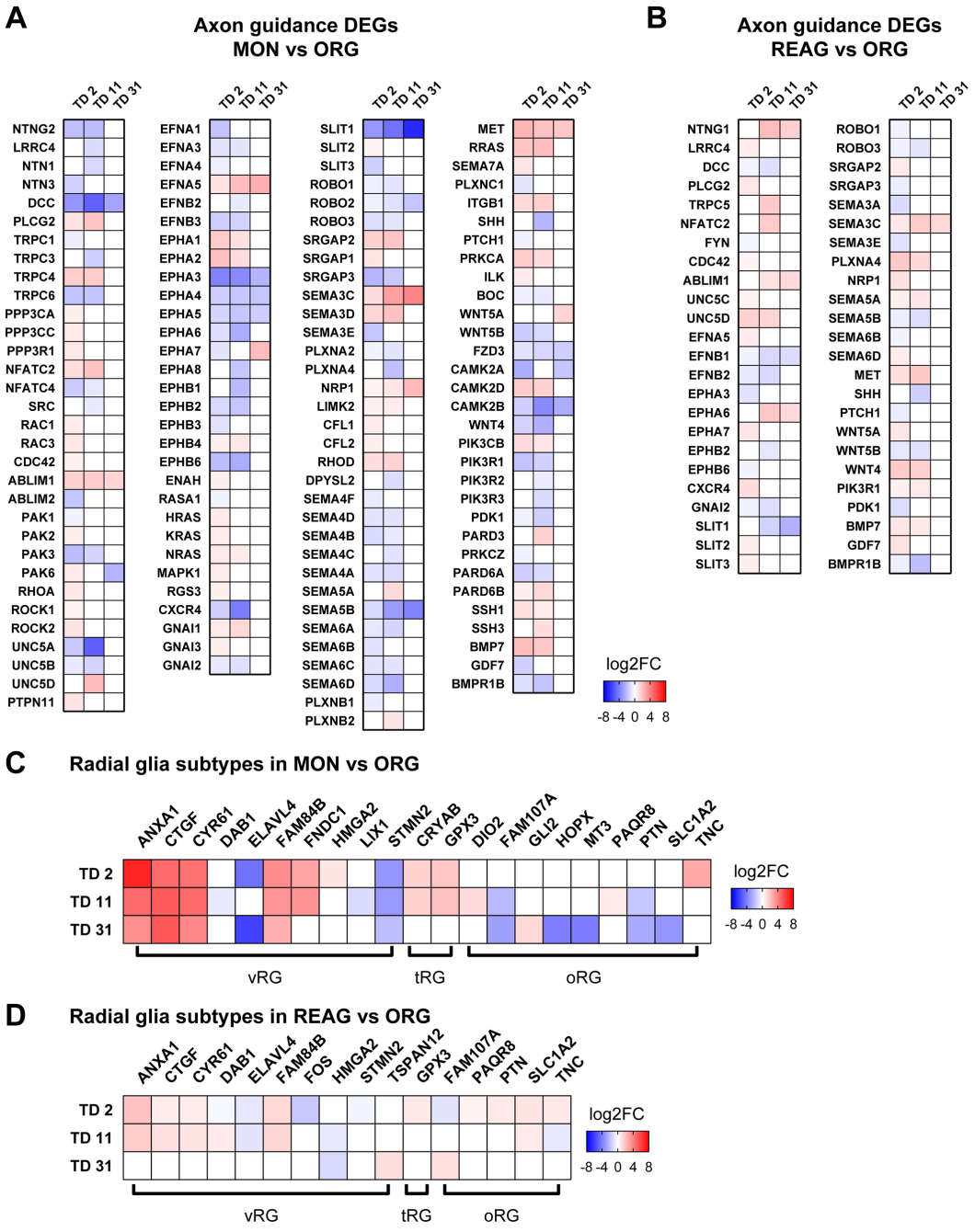

Figure S3. (A-B) Heat map of genes in the *Axon guidance* sublist (**Table S4b**) differentially expressed (log2 fold change values, FDR<0.05) between MON vs ORG (A) and REAG vs ORG (B) at least at one time point analyzed. **C-D**) Heat map of genes that identify radial glial subtypes (vRG, ventricular radial glia; tRG, truncated radial glia; oRG, outer radial glia) differentially expressed (log2 fold change values, FDR<0.05) between MONvsORG and between REAGvsORG, at least at one time point (**TableS4a**). Related to **Figure 3** and **Table S4**.

Figure S4 (Related to Figure 4 and Table S4).

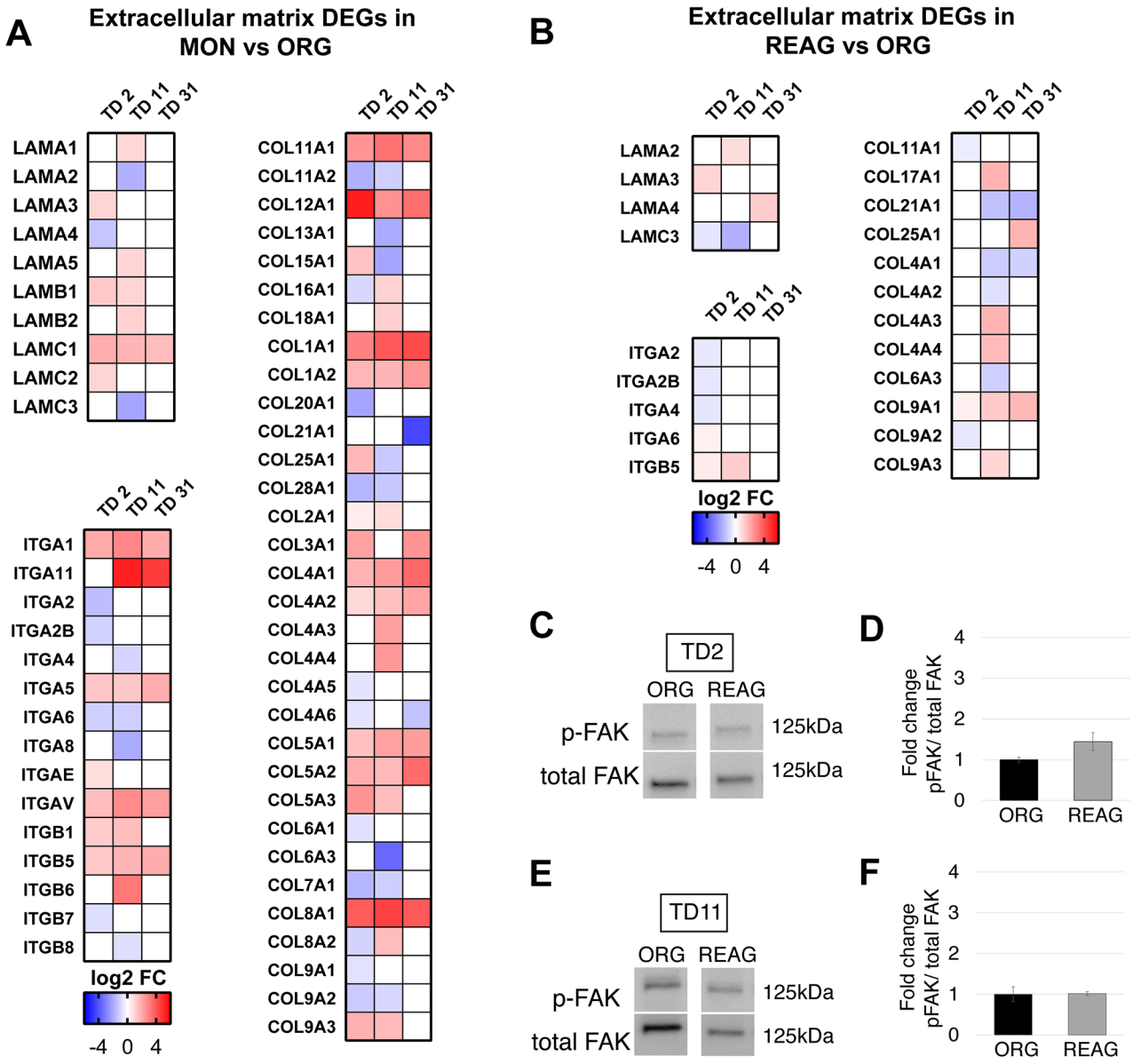

Figure S4. (A-B) Heat map of genes in the *Extracellular matrix* sublist (**Table S4d**) differentially expressed (log2 fold change values, FDR<0.05) between MON and ORG (A), or REAG vs ORG (B) at least at one time point analyzed. (**C-F**) Western blot analysis of phospho-FAK over total FAK protein expression in ORG and REAG at TD2 and TD11. Related to **Figure 4** and **Table S4**.

Figure S5 (Related to Figure 6).

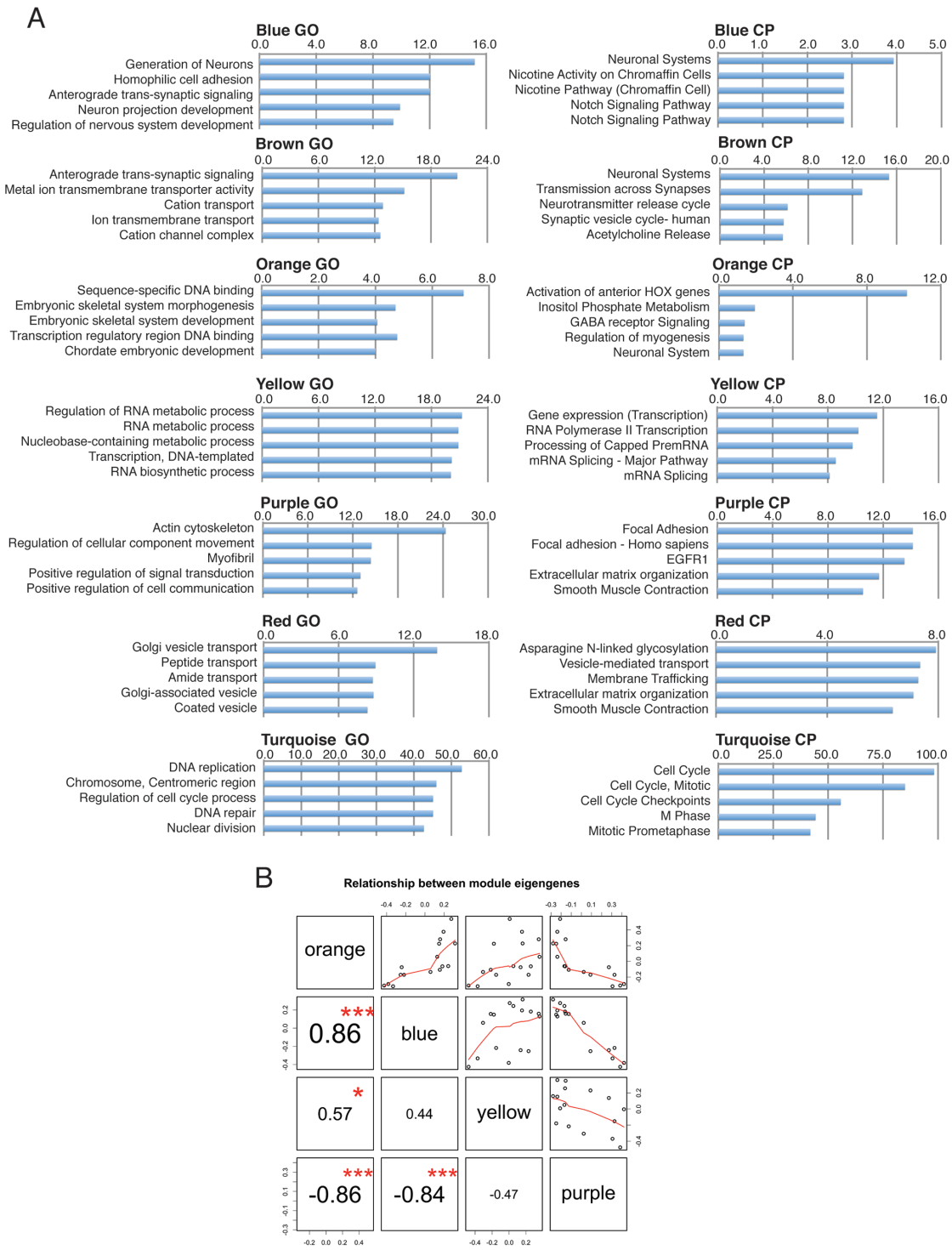

Figure S5. Characterization of the seven co-expression modules differentially expressed between ORG and MON. (**A**) Barplots of corrected p-values (expressed as –log10) for the top 5 Gene Ontologies (left) and Canonical Pathways (right) annotations. (**B**) Module to module eigenvalue correlation plots. Shown are the correlation coefficients and the associated significance. Related to **Figure 6**.

Figure S6 (Related to Figure 7).

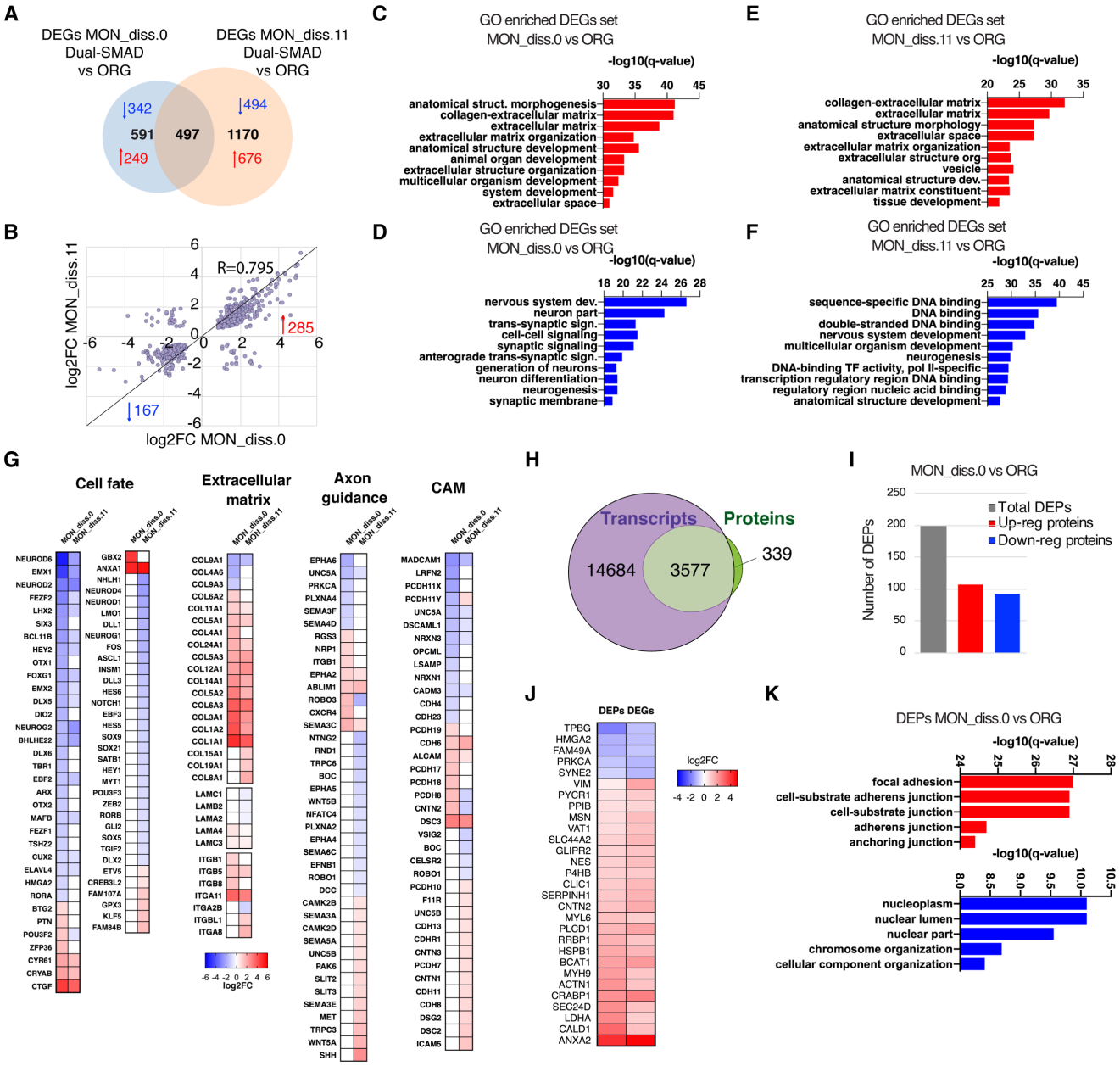

Figure S6. Consistency of transcriptomic changes in MON compared to ORG culture systems across different times of dissociation. (**A**) Venn diagram of total number of DEGs in early and late dissociated MON vs ORG. (**B**) Correlation plot of the shared DEGs in MON_diss.0 and MON_diss.11 compared to ORG. (**C-F**) Top GO-enrichment terms for up-regulated (red, C,E) and downregulated (blue, D,F) genes in early dissociated MON (C,D) and late dissociated MON (E,F). (**G**) Heat map of genes in the *neurodevelopmental genes list* differentially expressed (log2 fold change values, FDR<0.05) in MON_diss.0 and MON_diss_11 vs ORG. (**H**) Representation of the coverage and overlap between total identified transcripts and proteins in MON_diss.0 and ORG at TD25. (**I**) Number of differentially expressed proteins (DEPs) in MON_diss.0 vs ORG. (**J**) Heatmap of convergent DEPs and DEGs (log2 fold change values, FDR<0.05). (**K**) Top GO-enrichment terms for up- or down-regulated proteins in MON. Related to **Figure 7, Table S8.**

Supplemental Tables (uploaded as separate excel files)

Table S1. Metadata: list of all samples and experiments.
Table S2. Differential gene expression (DGE) analysis between time points in MON and ORG.
Table S3. Differential gene expression (DGE) analysis between MON and ORG at three time points, TD2, TD11 and TD31. Primer sequences used for qPCR validation of RNAseq data analysis.
Table S4. Neurodevelopmental genes list.
Table S5. Differential gene expression (DGE) analysis between REAG and ORG at three time points, TD2, TD11 and TD31.
Table S6. WGCNA analysis in MON and ORG samples at TD2, TD11 and TD31
Table S7. Transcription Factors Analysis results for the Blue module.
Table S8. Differential gene expression (DGE) analysis between early dissociated conditions (MON, REAG) and ORG, and late dissociated conditions (MON, REAG) and ORG at TD25. Proteomic analysis by LC MS/MS in early dissociated MON and ORG at TD25